

Evolution of Microstructure and Texture During Cold Rolling and Annealing of a Highly Cube-Textured ($\{001\}\langle 100 \rangle$) Polycrystalline Nickel Sheet

P.P. BHATTACHARJEE, Y. TAKATSUJI, Y. MIYAJIMA, D. TERADA, and N. TSUJI

The evolution of microstructure and texture is studied during the heavy cold rolling and annealing of a highly cube-textured ($\{001\}\langle 100 \rangle$) polycrystalline nickel sheet. Near and intermediate cube grains (≤ 5 deg and 5 deg to 10 deg misorientation, respectively, with exact cube orientation) are more unstable up to 60 pct reduction compared with the far cube grains (10 deg to 15 deg misorientation), and they rotate away to a rolling direction (RD)-rotated cube orientation ($\{013\}\langle 100 \rangle$, denoted by C_{RD}). In contrast, beyond 60 pct reduction, near and intermediate cube grains are more stable than far cube grains, which results in an overall increase in the stability of cube orientation. After 90 pct cold rolling, several cube bands adjacent to or surrounded by C_{RD} bands and separated by low-angle grain boundaries (LAGBs) over large part of their lengths are observed. After annealing of the 90 pct rolled material, no cube texture formation is observed, which is attributed to the delayed nucleation of cube grains owing to the unfavorable structure and local misorientation environment surrounding cube bands.

DOI: 10.1007/s11661-012-1093-9

© The Minerals, Metals & Materials Society and ASM International 2012

I. INTRODUCTION

THE recrystallization of heavily deformed metallic materials is often accompanied by the development of prominent crystallographic textures. The formation of sharp cube texture ($\{001\}\langle 100 \rangle$) in medium-to-high-stacking fault energy (SFE) face-centered cubic (fcc) materials (*e.g.*, Al, Cu, Ni, *etc.*) after heavy cold rolling and recrystallization is a well-known example of such recrystallization texture.^[1,2] The origin of cube texture has attracted considerable research interest because it can exert significant influence on a wide range of material properties including deep drawing properties of aluminum alloys for beverage can applications^[2] and critical current density of epitaxial high-temperature superconductor film grown on cube-textured nickel substrates.^[3]

The origin of cube texture is particularly intriguing because neither the orientation distribution function (ODF) nor pole figure analyses show any significant presence of the cube component in heavily deformed materials, although the cube component is the most

dominant texture component in the primary recrystallization texture of medium to high-SFE materials.^[2] Two different models, namely oriented nucleation (ON) and oriented growth (OG), depending on the relative contribution of the nucleation and growth stages of recrystallization, have been proposed and debated for a long time to explain the origin of sharp cube texture.^[4] In the oriented nucleation model, it is believed that the origin of cube texture is a result of the preferred nucleation of cube grains from the preexisting cube-oriented regions in deformed microstructure, which have been termed “cube bands.” The existence of such long, thin cube bands has been reported in many publications.^[5–7] When stated mathematically, the oriented nucleation factor (α) which is the ratio between the fraction (by number) of grains of a specified orientation (α_c) and the fraction expected in a random grain structure (α_r) must be larger than unity (*i.e.*, $\alpha = \alpha_c/\alpha_r \gg 1$).

In contrast, the oriented growth mechanism argues that the origin of sharp cube texture is the selective growth of the cube nuclei from a spectrum of available nuclei in the deformed material. The selective growth of cube grains is attributed to the high-mobility misorientation relationship, such as 40 deg $\langle 111 \rangle$, existing between the cube orientation and a major component of deformation texture such as the S component ($\{123\}\langle 634 \rangle$). The oriented growth factor (β), which is the ratio between the average grain diameter of the cube (d_{cube}) and off-cube ($d_{\text{off-cube}}$) grains, must be larger than unity (*i.e.*, $\beta = d_{\text{cube}}/d_{\text{off-cube}} \gg 1$). Doherty^[8] showed that the nucleation factor α and growth factor β might be measured through electron backscatter diffraction (EBSD), which greatly facilitates the quantitative analysis. Although the mechanism of formation of cube texture is not yet conclusive, recent studies have favored

P.P. BHATTACHARJEE, Assistant Professor, is with the Department of Materials Science and Engineering, Indian Institute of Technology Hyderabad, Ordnance Factory Estate, Yeddumailaram AP 502205, India. Contact e-mail: pinakib@iith.ac.in Y. TAKATSUJI, Undergraduate Student, D. TERADA, Assistant Professor, and N. TSUJI, Professor, are with the Department of Materials Science and Engineering, Graduate School of Engineering, Yoshida Honmachi, Sakyo-Ku, Kyoto 606-8501, Japan. Y. MIYAJIMA, Assistant Professor, is with the Department of Materials Science and Engineering, Interdisciplinary Graduate School of Science and Engineering, Tokyo Institute of Technology, Yokohama 226-8502, Japan.

Manuscript submitted August 28, 2011.

Article published online February 25, 2012

a more dominant role of ON than OG in the formation of sharp cube texture.^[2]

A major issue in the ON theory is the origin of preexisting cube-oriented regions in the deformed material. It has been argued that cube-oriented regions might originate by rotational mechanisms^[9,10] or they could originate from the initial cube-oriented grains present in the starting hot-rolled materials,^[11] even though slight deviations from the exact cube orientation will lead to instability and cube orientation will rotate away to other orientations gradually, as shown theoretically by Klein and Bunge^[12] and as supported by several other experimental studies on cube-oriented single crystals of different materials.^[13,14]

In contrast to studies on single crystals with cube orientation,^[13,14] the deformation and recrystallization behavior of cube grains in polycrystalline aggregates have hardly been studied systematically, although in few isolated cases, studies have been carried out on materials with relatively strong initial cube texture.^[15,16] One possible reason could be that usually, heavy deformation (≥ 90 pct) is needed for the formation of a strong cube texture during subsequent annealing, and as a result, the thickness of the resultant strips might be too thin for subsequent cold rolling. The current work attempts to study the evolution of microstructure and texture during heavy cold rolling and recrystallization of a near 100 pct cube textured polycrystalline nickel sheet processed by accumulative roll bonding (ARB), which is a well-known severe plastic deformation technique.^[17] Because of the nature of the ARB process, large plastic strain might be imparted, keeping the thickness of the sheet constant during the processing cycle. On subsequent annealing, a strong cube texture can form,^[18] and at the same time, the thickness of the tape remains suitable for subsequent cold rolling without necessitating any special requirements. Because most grains in such a starting material are cube oriented, it is much more convenient to study the microstructure and texture changes systematically with progressing deformation that might yield valuable information concerning the stability of cube grains in polycrystalline aggregates during cold rolling and its effect on the formation of recrystallization texture during subsequent annealing. These issues are the subjects to be clarified in this investigation.

II. EXPERIMENTAL

The starting material for the current work, a highly cube-textured polycrystalline nickel sheet (~ 99.7 pct purity), was prepared through severe plastic deformation (SPD) by ARB to an accumulated strain value of 6.4 (corresponding to ~ 99.7 pct reduction in thickness) followed by annealing at 1073 K (800 °C) for 1 hour in a salt bath furnace. The detailed experimental procedure has been given elsewhere.^[18]

The cube-textured polycrystalline nickel sheet was subsequently cold rolled with lubrication at room temperature to various reductions in thickness, namely, ~ 18 pct, 40 pct, 60 pct, 80 pct, and 90 pct (corresponding

to true strain $[\epsilon]$ values ~ 0.20 , 0.51, 0.92, 1.6, and 2.3, respectively) up to a final thickness of $\sim 100 \mu\text{m}$, using a laboratory scale, four-high rolling equipment with a work roll of 30 mm and back-up roll of 70 mm diameter. The 90 pct cold-rolled material ($\epsilon = 2.3$) was recrystallized subsequently for 1 hour in salt bath furnaces maintained at 623 K (350 °C), 873 K (600 °C), and 1073 K (800 °C). To study the early stages of nucleation, few cold-rolled samples were recrystallized partially at 623 K (350 °C) for 90 seconds. All the heat-treated samples were quenched immediately in cold water after the heat treatment.

The microstructure and texture of the materials were characterized mainly by using automated EBSD system attached to a FEI-SIRION (FEI Company, Hillsboro, OR) scanning electron microscope (SEM) equipped with field-emission gun. TSL-OIM software (EDAX Inc., Mahwah, NJ) was used for the analysis of the acquired EBSD data. The samples for EBSD measurements were prepared by mechanical polishing followed by electropolishing at an ambient temperature using a mixture of acetic and perchloric acids (19:1 by volume) as the electropolishing reagent. A cutoff angle of 15 deg was used for calculating the volume fraction of different texture components from the EBSD data.

III. RESULTS

A. Microstructure and Texture Evolution During Deformation

Figure 1 shows the microstructure and texture of the starting cube-textured polycrystalline nickel sheet obtained through the ARB and annealing process mentioned previously. The cube grains in the orientation map in Figure 1(a) have been highlighted in different colors depending on their misorientation from the exact

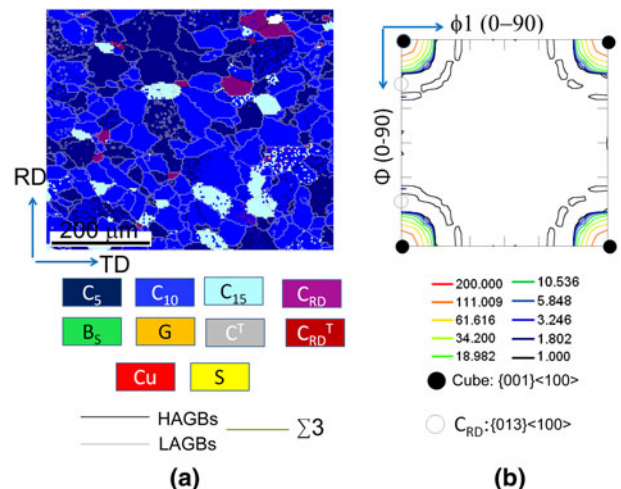


Fig. 1—(a) Orientation map and (b) $\Phi_2 = 0$ deg section of the ODF of the starting highly cube-textured polycrystalline nickel sheet. The color codes for the maps and intensities of the contour lines shown hereafter are same as those in Fig. 1. The exact location for the cube and C_{RD} orientations are shown by filled and open circles, respectively, in the $\Phi_2 = 0$ deg section of the ODF in (b) (Color figure online).

cube orientation. The fraction of near cube grains (defined as the grains within 5 deg misorientation with the exact cube orientation and are denoted as C_5 ; highlighted in deep blue in Figure 1(a)) is 35 pct of the whole observed area, whereas those of the intermediate cube grains (defined as the grains with misorientation between 5 deg and 10 deg with the exact cube and are denoted as C_{10} ; highlighted in blue in Figure 1(a)) and far cube grains (defined as the grains having misorientation between 10 deg and 15 deg with the exact cube and are denoted as C_{15} ; highlighted in light blue in Figure 1(a)) are ~56 pct and 7 pct, respectively. The volume fraction of the rotated cube grains (denoted as $\{013\}\langle 100\rangle$, which is obtained by rotating the cube orientation by 19 deg around the rolling direction [RD]; highlighted in purple in the orientation map in Figure 1(a)) is 1.7 pct. Brass or B_S ($\{110\}\langle 112\rangle$, highlighted in green), S ($\{123\}\langle 634\rangle$, highlighted in yellow), copper or Cu ($\{112\}\langle 111\rangle$, highlighted in red), and Goss or G ($\{110\}\langle 001\rangle$, highlighted in orange) orientations are completely absent in the annealed material. The microstructure is almost twin free so that the twin of cube or C^T ($\{221\}\langle 122\rangle$, highlighted in light gray) and twin of C_{RD} or C_{RD}^T ($\{185\}\langle 212\rangle$, highlighted in deep red) orientations are not observed in the microstructure. It might, thus, be understood clearly that the starting material is almost fully cube textured (~98 pct), and few grains have a rotated cube or C_{RD} orientation. This is also easily confirmed from the $\Phi_2 = 0$ deg section of the ODF of this starting material (Figure 1(b)), which reveals high intensity around the exact cube location at four corners of the ODF section. Because of the presence of the extremely sharp cube texture, the grain boundary network consists predominantly of low-angle grain boundaries (LAGBs; highlighted in light gray and defined as those with a misorientation $[\theta]$ of $2 \text{ deg} \leq \theta \leq 15 \text{ deg}$). High-angle grain boundaries (HAGBs; highlighted in black and defined as those with $\theta > 15 \text{ deg}$) and annealing twin or $\Sigma 3$ boundaries (highlighted in dark yellow) are found to be almost absent in the microstructure.

Figure 2 shows the gradual evolution of microstructure and texture in the cube-oriented polycrystalline nickel sheets with increasing cold-rolling reduction. All the EBSD maps have been acquired from the normal direction (ND)-RD plane (normal to transverse direction (TD)) of the sheets. The volume fractions of individual texture components at different stages of cold rolling are shown in Figure 3. After 18 pct cold rolling (Figure 2(a)), the recrystallized grain structure of the starting material (Figure 1(a)) could still be observed. However, the volume fractions of various texture components compared with the starting polycrystalline nickel sheet are found to be altered (Figure 3). The C_5 and C_{10} fractions are 12 pct and 53 pct, respectively, in the 18 pct cold-rolled condition. These values indicate a significant decrease in the volume fraction of C_5 and C_{10} components from the starting material (Figure 3). In contrast, the C_{15} fraction after 18 pct rolling is ~19 pct (Figure 3), indicating a massive increase from just 5 pct in the starting material. The total volume fraction of the cube component (~68 pct) or C_{total} ($C_{\text{total}} = C_5 +$

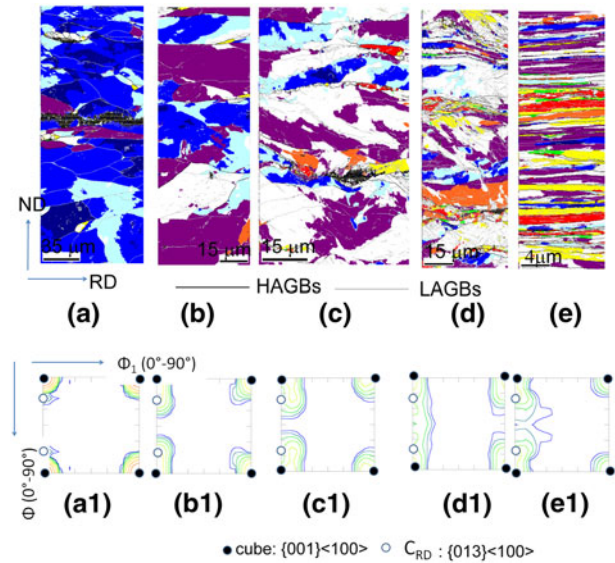


Fig. 2—EBSD orientation and grain boundary maps of (a) 18 pct, (b) 40 pct, (c) 60 pct, (d) 80 pct, and (e) 90 pct cold-rolled materials. (a1 to e1) are the corresponding $\Phi_2 = 0$ deg section of the ODFs (Color figure online).

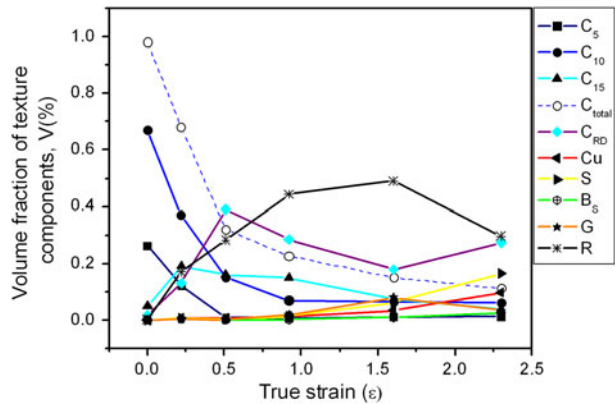


Fig. 3—Volume fraction of various texture components in the Ni sheets at different stages of cold rolling.

$C_{10} + C_{15}$) decreases significantly compared with the starting material (~98 pct), which is shown in Figure 3. The decrease in the volume fraction of C_{total} is compensated mostly by an increase in the volume fraction of the C_{RD} component, which changed from 1.7 pct in the starting material to 13 pct in the 18 pct rolled material (Figure 3). A significant increase in the random or R fraction (random components are all other components excluding those highlighted in the orientation maps, namely cube, C_{RD} , Cu, S, B_S , G, C^T , and C_{RD}^T , and those shown in white in the orientation maps) could also be noticed (Figure 3). The typical fcc rolling texture components such as Cu (highlighted in red), S (highlighted in yellow), B_S (highlighted in green), and G (highlighted in orange) have negligible presence in this condition (Figure 2(a)). The texture after 18 pct cold rolling is dominated by the cube component, which is understood clearly from the $\phi_2 = 0$ deg section of the ODF (Figure 2(a1)). The scatter around the cube

component along the Φ axis, which is not observed in the starting material (Figure 1(b)), confirms the development of the C_{RD} component.

After subsequent cold rolling to 40 pct reduction in thickness, the microstructure seems to be somewhat flattened along the RD (Figure 2(b)). It might be noteworthy that in a single cube grain, different regions appear with different misorientation from the exact cube orientation, which indicates clearly the process of fragmentation of cube grains. The C_5 and C_{10} fractions are found to be 0.9 pct and 15 pct, respectively, which indicates a subsequent decrease of these components compared with the 18 pct rolled material (Figure 3). The C_{15} fraction decreases to 16 pct. The C_{total} fraction in this condition is 32 pct, which suggests a large decrease compared with the 18 pct rolled material. In contrast, the C_{RD} fraction is 39 pct, which indicates a subsequent increase compared with the 18 pct rolled material. Cu, S, and B_S orientations exist only in negligible proportions in this deformed condition. However, the R fraction increases to ~ 28 pct. Thus, the decrease in the volume fraction of the cube grains is compensated mostly by the increase in the volume fractions of C_{RD} and R components. The $\Phi_2 = 0$ deg section of the ODF (Figure 2(b1)) in this deformed condition amply corroborates this observation.

After subsequent cold rolling to a 60 pct reduction in thickness, the C_5 fraction becomes almost negligible (0.7 pct), whereas the C_{10} and C_{15} fractions decrease to 7 pct and 10.5 pct, respectively. The C_{total} fraction in this condition is only ~ 18 pct. The C_{RD} fraction (~ 28 pct) is also found to decrease considerably compared with the 40 pct rolled material. The $\varphi_2 = 0$ deg section of the ODF (Figure 2(c1)) in this deformed condition also indicates the presence of some amount of ND-rotated cube component alongside the C_{RD} component. S (1.3 pct)-, Cu (1.3 pct)-, and G (1.8 pct)-oriented regions appear in the orientation map (Figure 2(c)), but the volume fractions are still found to be small. In contrast, a large volume of deformed material in this condition is found to have random (R) orientations (49 pct).

The C_5 fraction (1.1 pct) shows a slight increase after subsequent cold rolling to an 80 pct reduction in thickness. C_{10} fraction (6.2 pct) decreases slightly compared with that in the 60 pct rolled material, whereas the C_{15} fraction is 7.3 pct, indicating a relative decrease compared with the 60 pct rolled material. The C_{total} fraction in this condition is ~ 15 pct. The presence of C_{RD} is noticed in the orientation map (Figure 2(d)) and in the ODF (Figure 2(d1)). The volume fraction of this component is ~ 18 pct. The R fraction remains more or less similar to that in the 60 pct rolled material. The microstructure in this condition (Figure 2(d)) is also characterized by noticeable presence of S (6.2 pct) and G (7.9 pct), as well as a minor presence of the Cu (3.3 pct) and B_S (0.9 pct) components.

A clear lamellar structure typical in heavily cold-rolled material^[19] evolves after subsequent cold rolling to a 90 pct reduction in thickness (Figure 2(e)). The key microstructural parameters to define such deformed lamellar structures adequately, such as HAGB fraction (f_{HAGB}), HAGB spacing along the ND (d^{HAGB}), and

average misorientation angle, are determined from the EBSD data and are found to be 42 pct, 0.65 μm , and 19 deg, respectively. The large cube or C_{RD} -oriented bands parallel to RD are clearly visible in the orientation map and have an average thickness of 0.75 μm . The C_5 volume fraction (1.7 pct) in this condition is small but interestingly signifies a relative increase compared with the 80 pct rolled material. The C_{10} and C_{15} fractions are 6.2 pct and 3.8 pct, respectively. These values indicate a relative decrease compared with those in the 80 pct rolled material. The C_{total} fraction is 11.7 pct in the 90 pct cold-rolled material. The C_{RD} component persists, as observed from the orientation map in Figure 2(e) (C_{RD} fraction ~ 27.3 pct) and from the ODF (Figure 2(e1)). The R fraction is ~ 30 pct. A considerable presence of the Cu (~ 10 pct) and S (16.4 pct) components could be observed, whereas the B_S (2.4 pct) and G (3.3 pct) components are present in smaller proportions. Although deformation beyond this level has not been carried out in the current study, the increase in volume fractions of the typical fcc rolling texture components at this stage indicates the possibility of the development of typical fcc cold-rolling texture with subsequent deformation.

Figure 4(a) shows the structure of the cube bands in the 90 pct cold-rolled specimen in detail, and Figure 4(b) shows the point-to-point and point-to-origin (or accumulated) misorientations along the arrows in Figure 4(a) for different bands. Many of these cube-oriented bands in Figure 4(a) are found to be adjacent to or surrounded by the C_{RD} bands and separated by boundaries with relatively low misorientation over large part of their lengths. The point-to-point misorientation values for different bands do not show any significant difference and are typical for low-angle cell or subgrain boundaries (Figure 4(b)). The point-to-origin or accumulated misorientation for different bands seems similar and no significant accumulation of misorientation could be observed for any of these bands.

The misorientation environment in the deformed structure might be understood more thoroughly by comparing the local misorientation environment surrounding the cube bands and the bands of random orientations, respectively, in the form of discrete axis-angle misorientation plots as shown in Figure 5. A high density of points in the low misorientation range (0 to 15 deg) around the $\langle 100 \rangle$ misorientation axis is observed in the axis-angle misorientation plot of the cube bands (Figure 5(a)) presumably because of the presence of the C_{RD} (which is obtained by rotation of the cube orientation around $RD \parallel \langle 100 \rangle$) bands at the immediate neighborhood of the cube bands. In contrast, for randomly oriented bands, a high density of points is observed predominantly at high misorientation angle range (Figure 5(b)), clearly demonstrating high local misorientation environment for these randomly oriented bands.

B. Evolution of Microstructure and Texture During Annealing

Figure 6 shows the microstructure and texture in the 90 pct cold-rolled tapes after annealing at 623 K

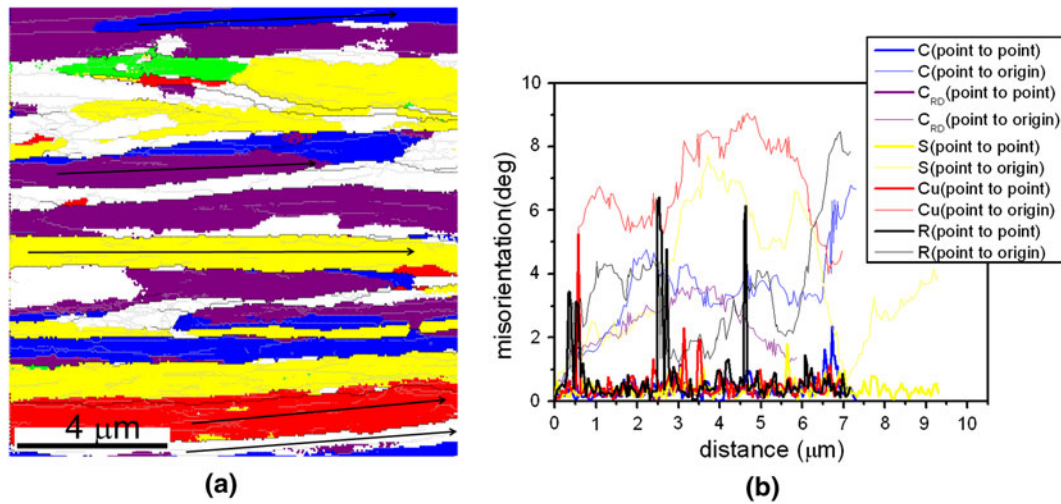


Fig. 4—(a) EBSD orientation and grain boundary map showing the detailed structure and misorientation environment surrounding cube bands in the 90 pct cold-rolled specimen. (b) The misorientation gradient inside the bands of different orientations.

(350 °C) for 1 hour. The microstructure indicates that the material is not recrystallized fully in this condition, which is also supported by the presence of a large fraction of LAGBs mostly in the regions with C or C_{RD} orientations (Figure 6(a)). Subsequently, the recrystallized regions are separated from the deformed regions applying an internal misorientation (documented as Kernel Average Misorientation [KAM] in the TSL-OIM software nomenclature^[20]) and grain size criterions. For recrystallized regions, the criteria are set as $KAM \leq 1$ and grain size (in area) $\geq 5 \mu\text{m}^2$. The recrystallized fraction is determined to be ~ 60 pct after this partitioning process. Evidently, most of the deformed regions in this annealed condition have predominantly cube or C_{RD} orientations (Figure 6(b)), which indicates that recrystallization of cube and C_{RD} orientations is suppressed greatly in this material. This observation is surprising considering that the cube regions are believed to recrystallize early in the annealing process, as observed in many previous publications.^[1,4] It must be noted that the current observation is in sharp contrast to numerous other observations that reported preferential nucleation of cube grains from cube-oriented regions in heavily deformed materials, and it remains a basic premise of the ON theory for explaining the formation of sharp cube texture. It should be noted that the big difference between the current study and previous investigations is in the microstructure and texture of the starting material.

Figures 7(a) and (b) show the orientation maps of the 90 pct deformed tape after subsequent annealing at 873 K (600 °C) and 1073 K (800 °C) for 1 hour, whereas Figure 7(c) and (d) show the corresponding $\Phi_2 = 0$ deg sections of the ODFs. The C_{total} fraction is only ~ 1 pct after annealing at 873 K (600 °C) (Figure 7(a)). The cube fraction increases slightly to ~ 3 pct after annealing at 1073 K (800 °C) (Figure 7(b)). Thus, it is concluded that cube texture formation is not observed in the current Ni sheets after annealing at different temperatures, which is also supported from the

$\Phi_2 = 0$ deg sections of the ODFs in these two annealed conditions (Figure 7(c) and (d), corresponding to 873 K (600 °C) and 1073 K (800 °C) annealed conditions, respectively), although a large fraction of the cube-oriented regions exists in the deformed microstructure.

C. Nucleation of Recrystallization and Evolution of Recrystallization Texture

It is surprising that cube texture does not develop in the heavily deformed sheets followed by annealing at different temperatures (Figures 6 and 7), although a significant presence of the cube-oriented regions could be confirmed in the deformed microstructure (Figure 3). The orientation map of the material annealed at 623 K (350 °C), however, indicates that the recrystallization of cube grains might be significantly delayed, which seems to be a possible reason for the observed behavior. However, because after annealing at 623 K (350 °C) for 1 hour the material is already at an advanced stage of recrystallization (~ 60 pct recrystallized), it would be necessary to observe the early stages of recrystallization and to determine the orientations of the early recrystallized grains. To achieve this, the 90 pct cold-rolled sheet was annealed slightly at 623 K (350 °C) for 90 seconds to yield a small recrystallized volume fraction. Because recrystallization occurred heterogeneously, several EBSD scans were conducted at different locations in the partially recrystallized material in which the average recrystallized fraction is determined to be ~ 5 pct.

Figure 8(a) shows a region of interest containing distinct, recrystallized grains appearing in clusters surrounded by deformed (unrecrystallized) regions. Subsequently, the recrystallized areas are separated from the deformed regions applying the conditions already mentioned and are shown in Figure 8(b). It is observed clearly from the orientation map of the recrystallized area (Figure 8(b)) that most of the early recrystallized grains do not have cube orientation, which is also corroborated amply by the $\Phi_2 = 0$ deg section of the

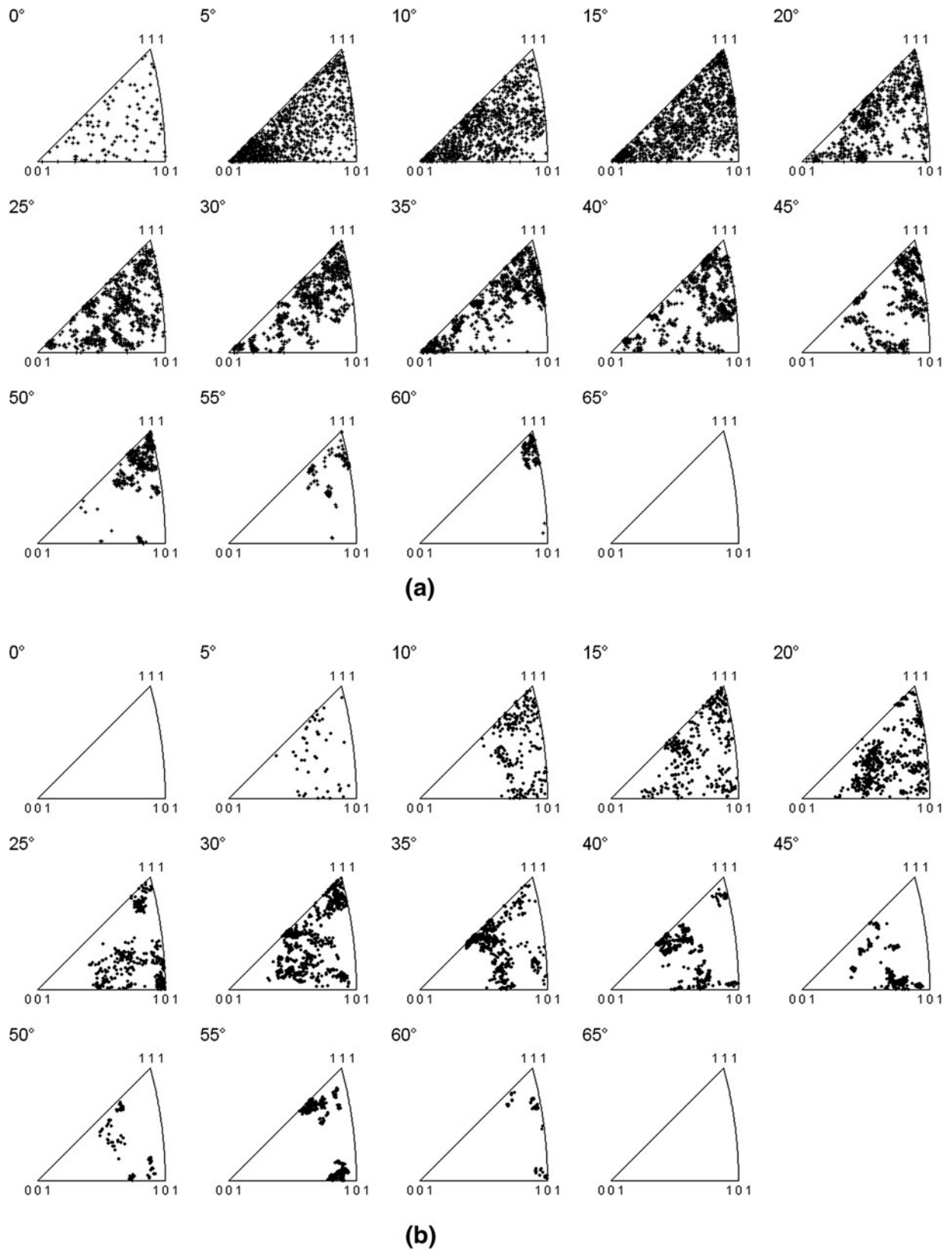


Fig. 5—Discrete angle-axis misorientation plots showing local misorientation environment of (a) cube and (b) randomly oriented bands.

ODF (Figure 8(c)) calculated from such newly recrystallized grains found in different regions of the partially recrystallized material. The intensity peaks appearing in

the $\Phi_2 = 0$ deg section are associated with the orientations $\{025\}\langle 26 - 5 2 \rangle$ and $\{013\}\langle 12 + 15 5 \rangle$, which may be considered as C_{RD} orientation rotated about the ND.

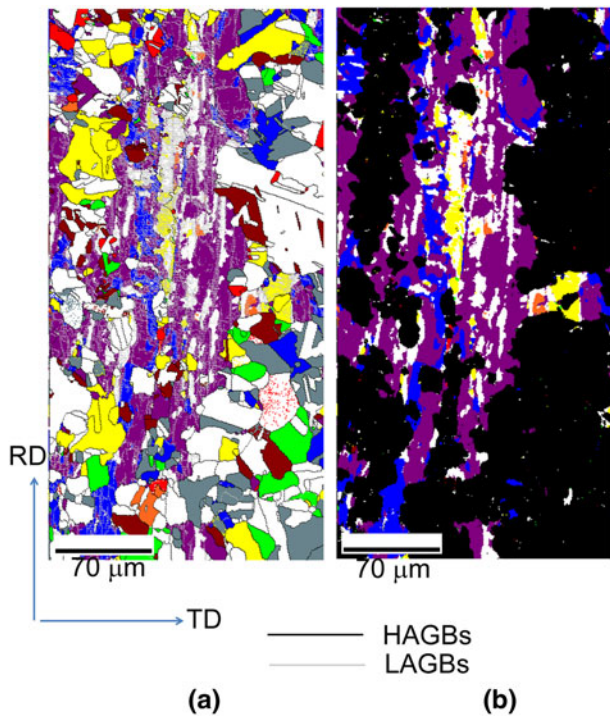


Fig. 6—(a) EBSD orientation and grain boundary map of the 90 pct cold-rolled material after annealing at 623 K (350 °C) for 1 h. (b) The orientation map showing the deformed (unrecrystallized) regions only.

Figures 9(a) and (b) are the orientation maps obtained from the same partially recrystallized material (90 pct cold-rolled sheet annealed at 623 K [350 °C] for 90 seconds) showing unrecrystallized cube-oriented regions. Figure 9(a) corresponds to the region marked by the dotted square in Figure 8(a). Figure 9(b) is obtained from the RD-TD (ND normal) plane section. As is observed in the case of the 90 pct cold-rolled material (Figure 2), the unrecrystallized cube regions in the partially recrystallized material are surrounded by C_{RD} -oriented regions and are separated by LAGBs over a large part of their length. It might be interesting to note that the cube-oriented regions in Figure 9(b) have a kind of “shell and core” structure in which inner core belongs to the near-cube orientation surrounded by the intermediate and far-cube oriented shells.

IV. DISCUSSION

A. Deformation Microstructure and Texture

The major observations concerning the stability of the cube grains during cold rolling in polycrystalline nickel sheet with strong initial cube texture can be summarized as follows:

- (a) The volume fraction of the cube component decreases consistently with increasing cold-rolling reduction. At low strain levels (≤ 40 pct reduction in thickness), the decrease in the volume fraction of the cube component is compensated by the increase in the C_{RD} and random orientations.

- (b) At low to medium strain levels (≤ 60 pct reduction in thickness), the rate of decrease in cube component is much faster than that at higher rolling reductions (≥ 60 pct reduction in thickness). At low to medium strain levels, C_5 and C_{10} fractions decrease significantly faster than C_{15} fraction. The converse is true for high strain regime where C_{15} fraction decreases faster than C_5 and C_{10} fractions.
- (c) Even after heavy cold rolling (~ 90 pct reduction in thickness), a finite amount of cube-oriented regions is retained in the form of elongated bands adjacent to or surrounded by C_{RD} -oriented bands.

The development of the C_{RD} component at the expense of cube component at low to medium strain levels indicates that initially, the cube-oriented grains rotate around the RD toward the C_{RD} orientation. This also seems to be the reason why many C bands after heavy cold rolling are found to be adjacent or surrounded by the C_{RD} bands (Figure 2). The current observations on the deformation behavior of the cube grains in polycrystalline aggregates are consistent with that of the cube-oriented (slightly misoriented from the exact cube orientation) nickel single crystal deformed to a similar strain level where the formation of a strong RD-rotated cube component has also been reported.^[14] This seems to occur through a process of grain subdivision during cold rolling where regions in a single-cube grain is subdivided into regions with different orientations as a result of different slip activities. This phenomenon can be understood clearly from the orientation maps of the 18 pct and 40 pct cold-rolled materials (Figure 2) in which different regions develop with different misorientation from the exact cube orientation all within a single-cube grain. Considering that the average grain size of cube grains is $\sim 45 \mu\text{m}$ in the starting material, the expected average cube grain thickness after 90 pct cold rolling should be $\sim 4.5 \mu\text{m}$, which is much larger than the observed average cube band thickness of $\sim 0.75 \mu\text{m}$ in the heavily rolled material. This finding indicates clearly that the initial cube grains in the starting material are fragmented considerably during the process of cold rolling.

Furthermore, a clear pattern is observed in the deformation process of cube grains, which depends on their misorientation from the exact cube location. The changes in the fractions of C_5 , C_{10} , and C_{15} components at different stages of rolling (Figure 3) suggest that initially, the C_5 and C_{10} grains are rotated away toward the C_{RD} orientation such that the volume fractions of these two components decrease quickly after just 18 pct cold rolling. Conversely, the C_{15} fraction actually increases in the initial stages of deformation, which indicates that some of the near and intermediate cube regions have rotated to the C_{15} orientation. After subsequent cold rolling to a 60 pct reduction in thickness, the largest decrease is observed in the case of C_5 and C_{10} orientations. The C_{15} fraction starts decreasing after 20 pct cold rolling but initially the rate of decrease is much smaller than the C_5 and C_{10} grains. In contrast, in the higher strain regime (≥ 60 pct reduction), the situation changes completely where the C_{15} fraction decreases

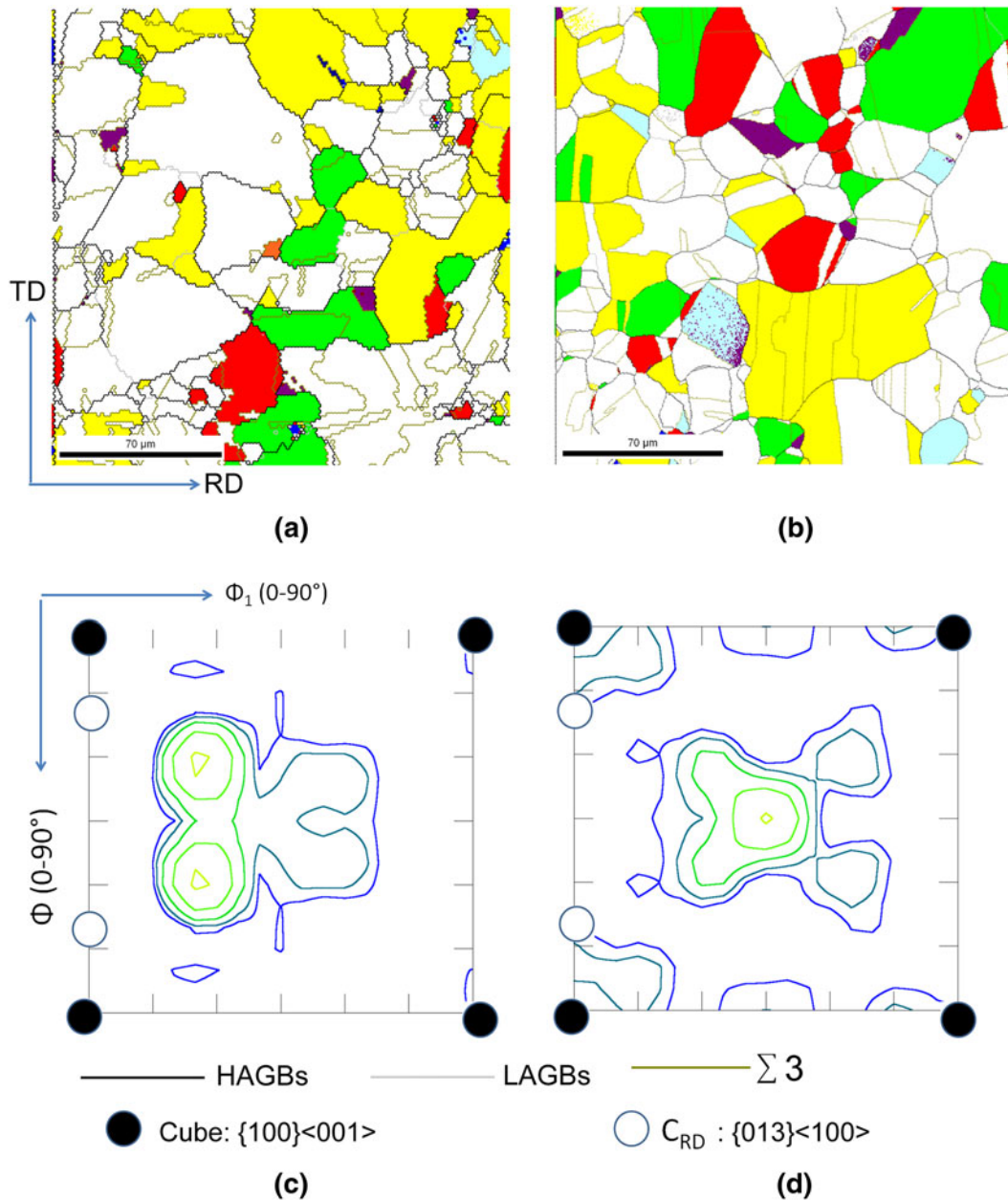


Fig. 7—EBSD orientation and grain boundary maps of the 90 pct cold-rolled material followed by annealing at (a) 873 K (600 °C) and (b) 1073 K (800 °C) for 1 h. (c and d) are the $\Phi_2 = 0$ deg sections of the corresponding ODFs. The color codes for the maps and intensities of the contour lines in the ODFs are same as those in Fig. 1.

faster than C_{10} fraction, and the C_5 fraction actually starts to increase, which indicates an increased stability of the C_5 and C_{10} orientations. It might be noted that (1) detailed measurements both carried out statistically in aluminum by Samajdar and Doherty^[21] and on individual grains studied by Doherty *et al.*^[22] in split channel die-processed samples before and after strain have also reported cube grain stability and (2) at the highest strains, near cube grains do rotate toward the exact cube orientation. These previous observations agree well with the cube stability reported in the current article.

The preceding pattern clearly suggests the existence of two-strain regimes for the stability of cube orientation, depending on the misorientation from the exact cube

location. In low-to-medium strain levels (≤ 60 pct reduction in thickness), the closer a grain to the exact cube location, the quicker it rotates away, whereas the more misoriented a cube grain is with the exact cube location, the more stable it is. In the higher strain regime, the behavior is the opposite. The remnant C_5 and C_{10} orientations become more stable against crystal rotation than the C_{15} orientation. It should be noted that this behavior does not agree with the theoretical calculations by Klein and Bunge,^[12] which predicts that the more misoriented a cube grain is with the exact cube location, the quicker it will rotate away.^[7] The observed differences in the theoretical calculations and the current experimental observations possibly indicate the complex

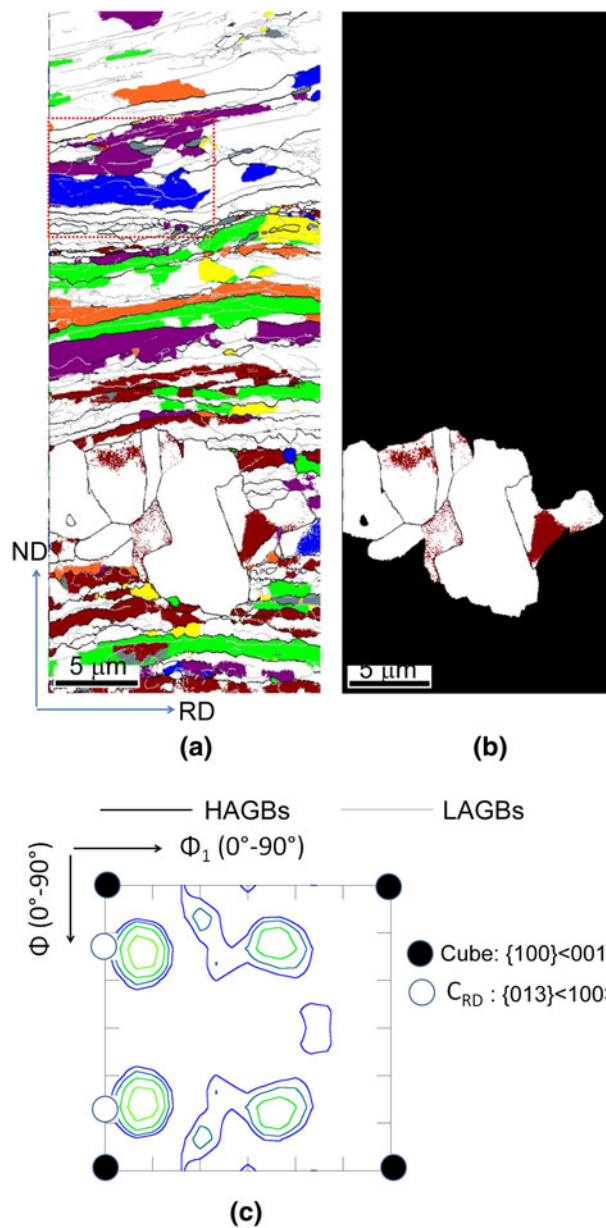


Fig. 8—(a) EBSD orientation and grain boundary maps of the 90 pct cold-rolled material followed by annealing at 623 K (350 °C) for 90 s. (b) The orientation map showing only the recrystallized areas in (a). (c) $\Phi_2 = 0$ deg section of the ODF calculated from the recrystallized areas in the partially recrystallized material. The color codes for the maps and intensities of the contour lines in the ODFs are same as those in Fig. 1.

deformation behavior of cube grains in a polycrystalline aggregate and need to be investigated in more detail.

The current observation that a significant amount of cube-oriented regions exist even after heavy cold rolling might be understood by observing the pattern in the relative change of C_{total} . Initially, the C_{total} fraction decreases fast, but beyond 60 pct cold rolling, the rate of decrease substantially slows down, which indicates an increased stability of cube orientation at higher strain levels because of the increased stability of the C_5 and C_{10} orientations as discussed previously. Although the deformation has not been carried out beyond 90 pct

reduction in thickness in the current study, this increased stability indicates a persistence of cube oriented regions even in heavily deformed materials observed here and reported in several articles.^[5–7]

The cube bands in the current case also have some prominent differences with such cube bands in other studies. Most notably, the cube bands are found adjacent to or surrounded by the C_{RD} regions (which has already been discussed) in the current study, and they do not have any internal misorientation gradient as has been reported in Ni-W alloy by Bhattacharjee *et al.*^[6] and in other publications.^[7] These characteristic differences observed in the current case seem to have important effects on the development of recrystallization texture, which will be discussed in the next section.

B. Nucleation of Recrystallization and Recrystallization Texture

The most interesting point in the results of this study is that no cube texture formation could be observed in the heavily (~90 pct) deformed material after annealing at different temperatures, although the deformed microstructure clearly shows a significant presence of cube-oriented regions (Figure 3). The microstructure after annealing at 623 K (350 °C) (Figure 6(a)) clearly shows deformed (unrecrystallized) cube regions surrounded by recrystallized grains with other orientations, which indicates clearly that the recrystallization of cube grains is inhibited greatly in the current case. This finding is supported also by the investigation on early stages of recrystallization (Figure 8) where most of the early recrystallized grains have a non-cube orientation and cube regions remain predominantly unrecrystallized (Figure 9). With the progress of recrystallization or after annealing at higher temperatures, the deformed cube regions are likely to be consumed by the growing recrystallized grains with non-cube orientations leading to the absence of cube texture, which is clearly observed in Figure 7.

The delayed recrystallization behavior of cube regions observed in the current study is in stark contrast with many previous studies that attribute strong cube texture formation to oriented or preferential nucleation of cube grains from the preexisting cube bands in the deformed microstructure at early stages of nucleation. The lack of a strong cube texture formation on recrystallization and at the same time a vanishingly small frequency of cube nucleation at early stages of recrystallization indicates clearly that an ON model of recrystallization texture is operating but in a negative sense. The delayed recrystallization behavior of the cube grains in the current case might be explained by the structure and local misorientation environment in the deformed condition. Generally, two conditions must be met for recrystallization to take place: Namely, a nucleus with a critical size and low dislocation density must be formed, and it should be bounded by HAGBs for subsequent growth. The attainment of critical size is favored by the presence of an orientation gradient by mechanisms such as rapid sub-boundary migration, and a recovered structure of cube regions because of a special arrangement of gliding

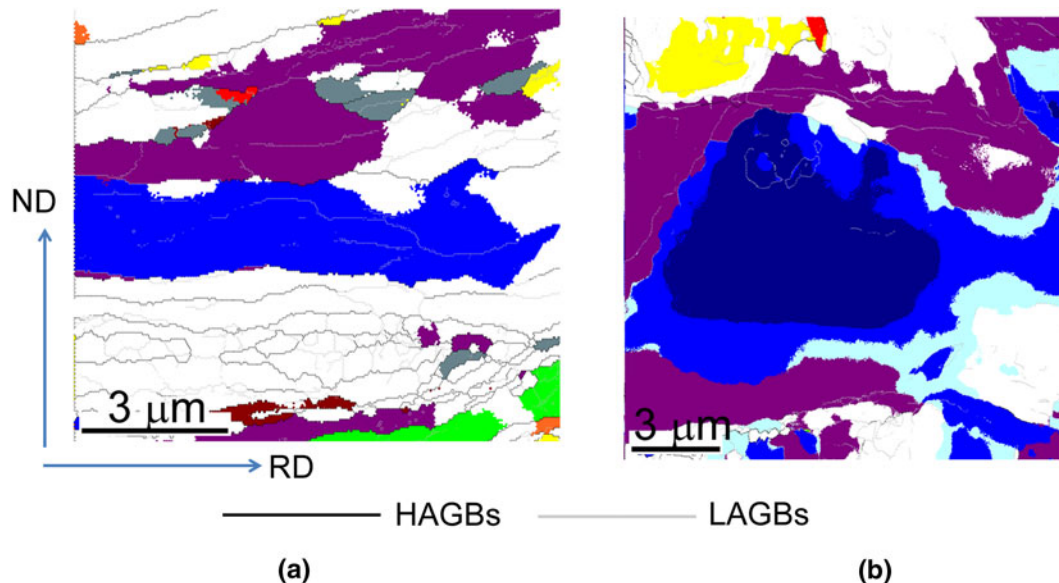


Fig. 9—EBSD orientation and grain boundary maps of the unrecrystallized cube regions in partially recrystallized condition obtained by annealing the 90 pct cold-rolled material at 623 K (350 °C) for 90 s. (a and b) are from the ND-RD and RD-TD sections of the partially recrystallized material, respectively.

dislocations as has been reported previously.^[5,7,18] In the absence of such a misorientation gradient, as observed in the current case, the nucleation would take place from small individual subgrains at the band boundaries.^[7] This requires a greater curvature and consequently more energy, thus making the nucleation of cube grains from the cube bands difficult in the current case. In addition, as has already been clearly seen, most of the cube bands are found adjacent to the C_{RD} bands or are surrounded by them; so that they separated from the C_{RD} bands by LAGBs over a large part of their length due to the mutual proximity of the two orientations leading to a low misorientation environment surrounding the cube bands (Figure 5(a)). This makes the cube bands unfavorable for nucleation. In contrast, randomly oriented bands have a more favorable nucleation environment as demonstrated clearly in Figure 5(b). This results in subsequent hindrance to the process of recrystallization of cube grains but relatively easier nucleation for randomly oriented bands, which agrees well with universally observed results that nucleation can only occur for a region that has a high local misorientation (typically greater than 15 to 20 deg). The current observation also differs with that of Doherty *et al.*,^[22] who explained that the absence of cube texture in the studies of Bolingbroke *et al.*^[15,16] was possibly because of orientation pinning. However, this study has direct evidence that the absence of cube texture after cold rolling and annealing of a highly cube textured nickel tape is the result of an unfavorable structure of the cube bands and low misorientation environment of cube bands with neighboring C_{RD} bands, which occurs because the nucleation of cube grains from the cube bands is hindered greatly. The absence of cube texture is not caused by the orientation pinning effect advanced by Doherty *et al.*^[1] If orientation pinning was operative, the cube grains would still nucleate from the cube bands and

grow into real recrystallized grains albeit with smaller than average size because of the impact of other cube bands spaced a small but finite difference away from the initial cube band.

Thus, it is understood clearly that unfavorable structure and local misorientation environment of the cube bands present in the heavily deformed material in this study impart significant hindrance to the recrystallization of cube grains, and as a result, strong cube texture formation is not observed in the current case after different annealing treatments. It may be noted that similar observations have been made during cold rolling and annealing of a cube-oriented single crystal of copper^[23] and also during the annealing of aluminum alloys with a strong initial cube texture after extensive, warm plane strain deformation.^[15,16] A large volume of cube-oriented regions could be detected in the microstructure after heavy cold rolling, but a weak cube texture formation is reported during annealing in these studies. Based on the current study, it seems that the origin of such a weak cube texture in the cold-rolled and annealed, cube-oriented, single crystal of copper and warm, plastic, strain-deformed aluminum with a strong initial cube texture could possibly be from the unfavorable misorientation environment in the deformed microstructures because of presence of C_{RD} bands adjacent to the cube bands. From this work, it is evident that the presence of cube-oriented regions in the microstructure of heavily deformed materials is not necessarily a sufficient condition for the formation of sharp cube texture after recrystallization. The internal structure and local misorientation environment surrounding the cube bands are far more important in the context of early nucleation of cube grains and subsequent formation of sharp cube texture during recrystallization.

V. CONCLUSIONS

The following major conclusions might be drawn from the results obtained in the current study using a highly cube-oriented polycrystalline Ni sheets as starting materials:

1. The initial cube grains of highly cube textured polycrystalline nickel sheet rotate about RD toward C_{RD} orientation during cold rolling up to a low-to-medium level of strain (≤ 60 pct reduction in thickness).
2. The rate of decrease of cube fraction is much higher below 60 pct reduction in thickness, but it diminishes beyond 60 pct rolling, indicating an increased stability of the cube component. This also explains the persistence of cube bands in heavily deformed materials as observed in the current case and often reported in the literature.
3. A significant amount of cube-oriented regions in the form of thin bands is retained in the deformed structure. The cube bands do not possess any significant misorientation gradient and frequently are found to be adjacent to the C_{RD} bands.
4. The stability of different cube orientations depends on the relative misorientation with the exact cube locations. Below 60 pct rolling, C_5 and C_{10} orientations are more unstable as compared to C_{15} orientations. In contrast, at high strain levels C_5 and C_{10} orientations show more stability than C_{15} orientation.
5. After annealing at different temperatures, no cube texture formation could be observed, although the heavily deformed material (~ 90 pct reduction) shows a significant amount of retained cube-oriented regions.
6. The absence of cube texture in the material after annealing seems to occur primarily because the nucleation of cube grains is inhibited greatly in this material, as indicated by the microstructure after low-temperature annealing at 623 K (350 °C) and the orientations of early recrystallized grains.
7. The absence of cube texture after annealing is attributed to the unfavorable structure and local misorientation environment surrounding the cube bands. An unfavorable structure and low misorientation environment created as a result of the presence of the C_{RD} bands adjacent to cube bands seem to be main reasons for inhibition of the nucleation of cube grains.
8. The current study demonstrates that the structure and local misorientation environment surrounding the cube bands in heavily deformed materials are much more important for the formation of cube

texture through oriented nucleation than the mere presence of large cube-oriented regions in the deformed microstructure.

ACKNOWLEDGMENTS

One author (P.P. Bhattacharjee) expresses his gratitude to the Japan Society for the Promotion of Science (JSPS), Japan and the Department of Science and Technology (DST), India for the award of DST-JSPS bilateral project (DST/INT/JSPS/P-114/2011).

REFERENCES

1. R.D. Doherty, D.A. Hughes, F.J. Humphreys, J.J. Jonas, D.J. Jensen, M.E. Kassner, W.E. King, T.R. McNelley, H.J. McQueen, and A.D. Rollett: *Mater. Sci. Eng. A*, 1997, vol. 238, pp. 219–74.
2. F.J. Humphreys and M. Hatherly: *Recrystallization and Related Annealing Phenomena*, 2nd ed., Elsevier, Oxford, U.K., 2004.
3. A. Goyal, M.P. Paranthaman, and U. Schoop: *MRS Bull.*, 2004, vol. 29, pp. 552–61.
4. R.D. Doherty: *Progr. Mater. Sci.*, 1997, vol. 42, pp. 39–58.
5. A.A. Ridha and W.B. Hutchinson: *Acta Metall.*, 1982, vol. 30, pp. 1929–39.
6. P.P. Bhattacharjee, R.K. Ray, and N. Tsuji: *Acta Mater.*, 2009, vol. 57, pp. 2166–79.
7. S. Zaefferer, T. Baudin, and R. Penelle: *Acta Mater.*, 2001, vol. 49, pp. 1105–22.
8. R.D. Doherty: *Scripta Metall.*, 1985, vol. 19, pp. 927–30.
9. I. Dillamore and H. Katoh: *Met. Sci. J.*, 1974, vol. 8, pp. 73–83.
10. T. Kamijo, H. Adachihara, H. Fukutomi, and E. Aernoudt: *Acta Metall. Mater.*, 1992, vol. 40, pp. 693–98.
11. H.E. Vatne, T. Furu, and E. Nes: *Mater. Sci. Technol.*, 1996, vol. 12, pp. 201–10.
12. H. Klein and H.J. Bunge: *Advances and Applications of Quantitative Texture Analysis*, H.J. Bunge, ed., DGM, Oberursel, Germany, 1989.
13. S. Kikuchi, E. Kimura, and M. Koiwa: *J. Mater. Sci.*, 1992, vol. 27, pp. 4927–34.
14. C. Hartig and M. Feller-Kniepmeier: *Acta Metall.*, 1985, vol. 33, pp. 743–52.
15. R.K. Bolingbroke, G.J. Marshall, and R.A. Ricks: *The Fourth Int. Conf. on Aluminum Alloys*, T. Sanders and E. Starke, eds., Georgia Institute of Technology, Atlanta, GA, 1996, p. 243.
16. R.K. Bolingbroke, G.J. Marshall, and R.A. Ricks: *Mater. Sci. Forum*, 1994, vols. 157–162, pp. 1145–51.
17. N. Tsuji, Y. Saito, S.-H. Lee, and Y. Minamino: *Adv. Eng. Mater.*, 2003, vol. 5, pp. 338–44.
18. P.P. Bhattacharjee and N. Tsuji: *Int. J. Mater. Res.*, 2011, vol. 102, pp. 173–82.
19. D.A. Hughes and N. Hansen: *Philos. Mag.*, 2003, vol. 83, pp. 3871–93.
20. S.I. Wright, D.P. Field, and D.J. Dingley: *Electron Backscatter Diffraction in Materials Science*, Academic/Plenum Publishers, New York, NY, 2000, pp. 141–52.
21. I. Samajdar and R.D. Doherty: *Acta Mater.*, 1998, vol. 46, pp. 3145–58.
22. R.D. Doherty, L.-C. Chen, and I. Samajdar: *Mater. Sci. Eng. A.*, 1998, vol. 257, pp. 18–36.
23. C.A. Verbraak: *Acta Metall.*, 1958, vol. 6, pp. 580–97.